Pre-calculation of time/current characteristics of "M"-effect fuse elements

M. Hofmann and M. Lindmayer

Abstract

A finite element method is used for a fuse element model and for the calculation of the time/current characteristic. The basic data which are needed for the calculation consist of material data (electrical conductivity, thermal conductivity, heat capacity, convection and radiation coefficients) and data which describe the dissolution processes related to the "M"-effect. The data concerning the dissolution behaviour between solder and fuse element metal were gained from micrographs of heat treated fuse elements. These fuse elements were exposed to different temperatures and times in a furnace in order to measure the dissolution depth. These dissolution process data were integrated into the program at each calculation time step.

The results of the calculation carried out for a Cu fuse element with tin solder show good agreement in a melting time range between 12 s and 200 min at overload currents.

1. Introduction

In "M"-effect fuses the dissolution of the base metal (Cu, Ag) by a deposit of soft solder is utilized to adjust the time/current characteristics in the overload range. The current heating of the fuse element causes melting of the solder spot and a dissolution process starts. This dissolution leads to a reduced cross section of the base metal. The dissolution behaviour is dependent of the load current because the effective remaining cross section, the resistance, the temperature and the dissolution velocity mutually influence and enhance each other. The fusing time lies in a range between some seconds and several hours.

Up to now no attempts to calculate the time/current characteristic in this time range are known.

Good solutions exist for the calculation of the time/current characteristics of fuse elements without "M"-effect for fusing times up to 100 seconds. Especially McEwan and Wilkins /1-3/ have done a lot of work in this field by using a finite difference method.

Earlier investigations /4/ with Cu fuse elements with Sn-solder spot showed that it is possible to calculate the dissolution depth when the fuse element is annealed at constant temperatures (without current load). Fig. 1 shows an example, the dissolution depth $\bar{x}$ starts at t = 0 with a steep increase and reaches a saturation value after some time. This saturation value can be derived from the saturation concentration for Cu in liquid Sn according to the liquidus line in the Cu-Sn phase diagram.

Other tests /5/ were performed with cyclic current load of Cu fuse elements with Sn solder. It was found that in each load cycle the dissolution only proceeds during the time span in which the maximum temperature of the preceding cycle is exceeded. This and the results of /4/ showed that the fuse element temperature is the ruling factor of the fusing behaviour caused by the "M"-effect.

Dipl.-Ing. M. Hofmann and Prof. Dr.-Ing. M. Lindmayer
Institut für Elektrische Energieanlagen
Technische Universität Braunschweig
D-3300 Braunschweig, Germany

The calculations of the time/current characteristic were carried out using the finite element program ADINAT /6/*.

The calculation is based on the heat flow equation:

$$\mathrm{div}\,(\lambda\cdot\mathrm{grad}\,T) = -q_G + c\,\frac{\partial T}{\partial t} \qquad (1)$$

The solution of this problem with the finite element method (FEM) leads to the variation-integral, which is solved by ADINAT:

$$\Pi = \int\limits_V \frac{1}{2}\cdot\lambda\cdot\left[\left(\frac{\partial T}{\partial x}\right)^2 + \left(\frac{\partial T}{\partial y}\right)^2 + \left(\frac{\partial T}{\partial z}\right)^2\right]\cdot dV - \int\limits_V T\cdot(q_G - c\cdot\frac{\partial T}{\partial t})\cdot dV + \int\limits_A T\cdot q_{ks}\cdot dA \qquad (2)$$

with:
Π variation integral
λ heat conductivity
T temperature
x,y,z coordinate axes
V volume
q_G internal generated heat per unit volume (ohmic heating of the fuse element)
c heat capacity per unit volume
t time
A surface
q_{ks} heat flow at surface A

q_G can be described by

$$q_G = j^2\cdot\rho\,(T) \qquad (3)$$

where j is the current density and $\rho(T)$ the temperature dependent specific resistance.

q_{ks} can contain a convection term q_k and/or a radiation term q_s.
q_k is defined by equation (4):

$$q_k = h\cdot(T_U - T) \qquad (4)$$

and q_s is analogous to equation (4):

$$q_s = \kappa\cdot(T_R - T) \qquad (5)$$

with:
h convection coefficient
κ radiation coefficient
T_U surrounding temperature
T_R temperature of external radiation sink
T element/node temperature

κ is defined by the following equation:

$$\kappa = \sigma\cdot\varepsilon\cdot f\cdot(T_R^2 - T^2)\,(T_R + T) \qquad (6)$$

---

* ADINAT (A Finite Element Program for Automatic Dynamic Incremental Non Linear Analysis of Temperatures) for the linear and nonlinear, steady state and transient finite element analysis of heat transfer - and temperature field problems in dependence of linear and nonlinear material properties.

with: σ Stefan-Boltzmann constant
ε emission factor
f form factor

2. Solution with the FEM-program ADINAT

ADINAT calculates the temperature distribution and the temperature/time curve respectively. The calculation is stopped when one of the following criteria is fulfilled:

a) The maximum fuse element temperature becomes greater than the melting temperature of the base metal.

b) The base metal beneath the solder is fully dissolved in the liquid solder at one place.

Fig. 2 shows a schematic diagram of the calculation.

The input block starts with the input of the control data (no. of nodes, element groups, time increment, starting time) and calculation data (convergence criterion, time integration method, etc.). Then the number of time increments, the nodal data, the starting conditions and the heat flow input data (esp. the time functions) are defined. The time functions describe the generated ohmic heat per volume $j^2 \cdot \rho(T)$ for every single element at all times and temperatures. The input block is terminated with the assignment of the material property data to the elements. The material property data (specific resistance, heat conductivity, heat capacity) were chosen according to fig. 3. The convection coefficient h (equation (4)) was chosen $h_0 = 1,2 \cdot 10^{-6}$ W/mm^2·K for the upper and side surfaces of the fuse element and $h_u = 6,5 \cdot 10^{-7}$ W/mm^2·K for the underside. Considering the Cu oxidation the emission factor was set to rise from $\varepsilon = 0,1$ to $\varepsilon = 0,6$ in a temperature range from 20 °C to 600 °C and $\varepsilon = 0,6$ at $T \geq 600$ °C. The form factor f (equation (6)) is set to 1 because all radiation is absorbed by the environment. At the fuse element terminals the temperature random condition is $T = \text{const} = 20$ °C.

The analyzing program integrates an additional iterative loop into ADINAT. This loop computes the correction of the time functions. The time functions, i.e. the generated power at each element, are not known at the start, because they are a function of the specific resistance ρ and hence of the temperature. The calculation therefore starts with estimated time functions. Each run of ADINAT yields the temporal and local dependence of the temperature. After each run the time functions are corrected according to the calculated temperatures in a loop outside ADINAT until a given temperature difference between two iterations is not exceeded. After this iteration the diffusion process at the solder is taken into account in a second loop outside ADINAT, as shown later.

3. Example: Cu fuse element without constriction/with Sn-solder surrounded by air

Fig. 4a shows the dimension of the simple straight fuse element, the test arrangement is described in /4/.

The FEM-model (fig. 4b) represents geometrically a quarter of the real fuse element. The asymmetric position of the solder is neglected, that means it is assumed that the solder is about 8 mm long. All elements range over the whole fuse element thickness.

The thickness dimensions of the solder area are relatively small, so it could be assumed that a fast heat balance within the solder and the base metal thickness occurs. Therefore in the solder area the electrically and thermally conducting path as well as the ohmic heat generation can be replaced by a body of a constant thickness equal to the base metal thickness, but with material data adjusted to the decreasing base metal and increasing solder cross section. In detail this is achieved as follows:

Estimations show that the current and heat flow within the original solder of thickness d_{Sn} can be neglected. Within the total base metal thickness (0.2 mm) there are two parallel paths consisting of the remaining copper of thickness $d_{Cu} - x$ and the dissolution depth x.

The equivalent electric resistivity then reads

$$\rho = \frac{\rho_x \cdot \rho_{Cu} \cdot d_{Cu}}{\rho_x \cdot (d_{Cu}-x) + \rho_{Cu} \cdot x} \qquad (7)$$

The heat conductivity and heat capacity are treated analogously.

Fig. 1 shows that the beginning of dissolution at a fixed temperature can be described by a nearly constant dissolution velocity. Assuming that no saturation occurs because of the steady increase of the resistance and the temperature the dissolution can be approximated by that value $v = dx/dt$ at $t = 0$. In fig. 5 this dissolution velocity is plotted as a function of temperature. Intermediate values are interpolated linearly between the measured values.

In the beginning the temporal and local temperature dependence is calculated without considering the dissolution. When the solder melting point is exceeded, an increase Δx in dissolution depth is calculated for each time step according to

$$\Delta x = v\ (T_{Solder}) \cdot \Delta t \qquad (8)$$

In the following time steps corrections of the materials properties and the watt losses in the solder area are made according to equation (7).

Fig. 6 is an example for such a calculation. In this case the initial transient heating which is short in comparison with the total fusing time was neglected. The temperature distribution at the beginning was assumed to have reached already equilibrium, hence the steady-state version of ADINAT could be used.

After switching on current the measured temperature at the solder increases within 1 minute to T = 335 °C, the melting point of Sn (232 °C) is reached already after t = 25 s. In a time range 1 min to 15 min the temperature increases only slightly from 335 °C to 400 °C. In this range the dissolution depth of the fuse element is relatively small (60 µm according to micrographs). At greater dissolution depth the changes in resistance become more important, so that the temperature, the resistance and the dissolution velocity enhance each other. Therefore a steep increase of the temperature occurs above 400 °C until the total copper thickness is dissolved. The measured temperature at this point is 740 °C, the melting point of Cu (1083 °C) is not reached. The measured fusing time is 20,6 min.

The result of the steady-state calculation at the beginning is a solder temperature of 330 °C, the further increase is a result of the stepwise dissolution calculation.

The total dissolution is reached after 21,6 min at T = 770 °C. The comparison shows a rather good agreement between measurement and calculation for the temperature-time dependence as well as for the fusing time.

Similar calculations were carried out for other currents. A result is the time/current characteristic (fig. 7). At I = 150 A, 160 A the fusing time becomes relatively small. Therefore the effect of the heat capacity was included in the calculation, which then takes into account the transient temperature rise. The agreement is generally good, except for 120 A. The deviation in terms of current is about 10 % in this area and below 3 % in the area around 100 A (fusing times around 1 to 3 hours).

Conclusions

The results show that it is possible to estimate the time/current characteristic of fuse elements with a solder spot by using a finite element method for the temperature field. The dissolution of the base metal into liquid solder is modelled by temperature-dependent dissolution velocity. The changing thickness of the base metal and solder respectively is replaced by appropriate material properties at the solder spot.

References

/1/ McEwan, P.M.: Numerical prediction of the pre-arcing performance of H.R.C. fuses
Thesis, Liverpool Polytechnic, 1975

/2/ Wilkins, R., McEwan, P.M.: A.C. short-circuit performance of notched fuse elements.
Proc. IEE 122 (1975), No. 3, p. 289-292

/3/ McEwan, P.M., Wilkins, R.: A decoupled method for predicting time-current characteristics of H.R.C. fuses
Int. Conf. on Electric Fuses and Their Applications, Liverpool, 1976

/4/ Hofmann, M., Lindmayer, M.: Fusing and ageing behaviour of fuse elements with "M"-effect at medium- and long-time overload
Int. Conf. on Electric Fuses and Their Applications, Trondheim, 1984

/5/ Hofmann, M., Lindmayer, M.: Alterungs-Verhalten von Sicherungsschmelzleitern bei zyklischen Überstrombelastungen
Int. Symp. on Switching Arc Phenomena, Lodz, 1985

/6/ - ADINAT - A Finite Element Program for Automatic Dynamic Nonlinear Analysis of Temperatures
Report AE 81-2 (1981)
ADINA Engineering AB, Västeras, Sweden

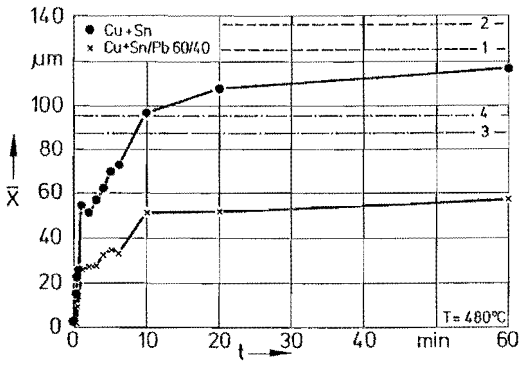

Fig. 1: Dissolution depth x as function of time t for different fuse elements

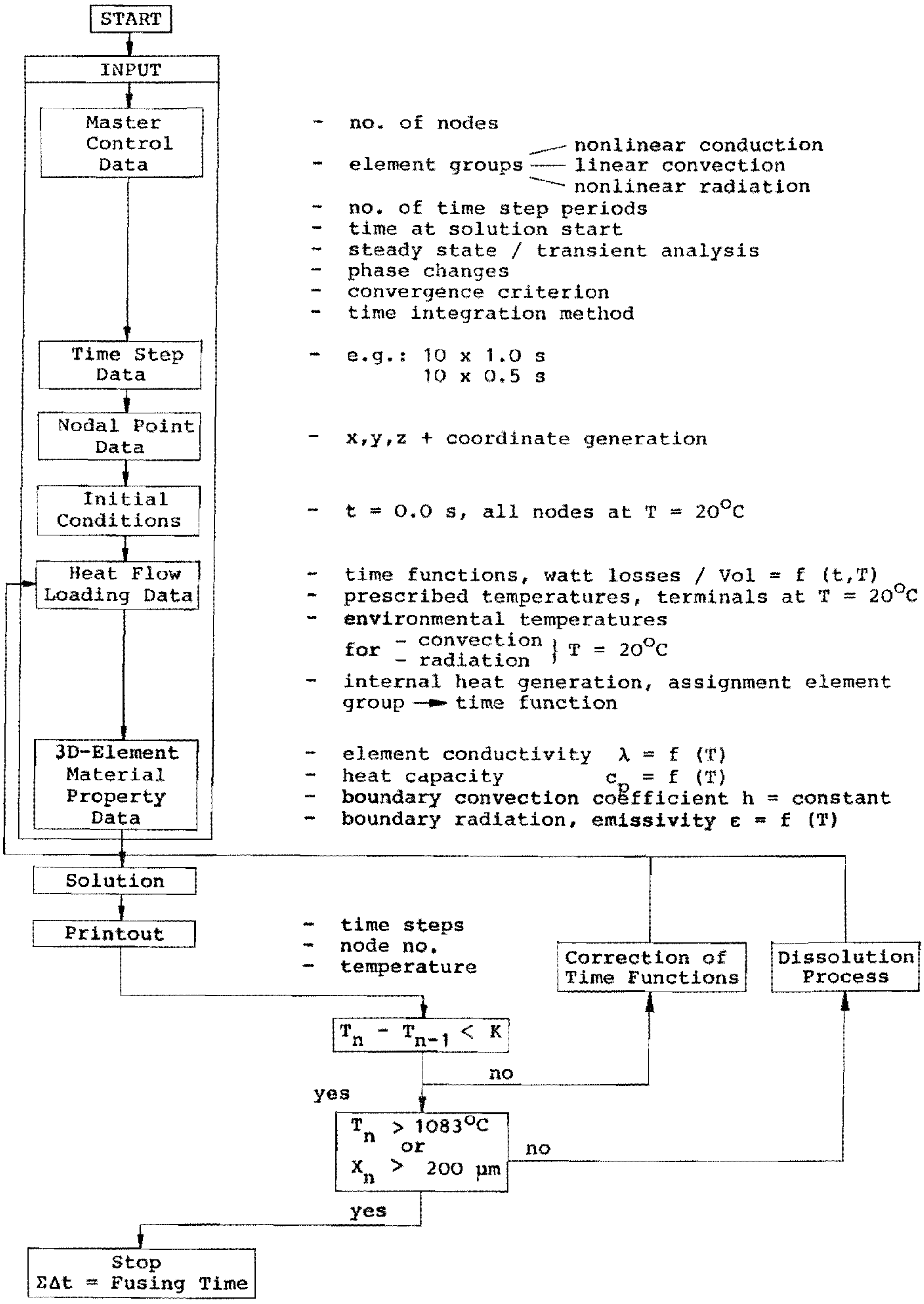

- no. of nodes
- element groups — nonlinear conduction / linear convection / nonlinear radiation
- no. of time step periods
- time at solution start
- steady state / transient analysis
- phase changes
- convergence criterion
- time integration method

- e.g.: 10 x 1.0 s
  10 x 0.5 s

- x,y,z + coordinate generation

- t = 0.0 s, all nodes at T = 20°C

- time functions, watt losses / Vol = f (t,T)
- prescribed temperatures, terminals at T = 20°C
- environmental temperatures for - convection, - radiation } T = 20°C
- internal heat generation, assignment element group → time function

- element conductivity $\lambda = f(T)$
- heat capacity $c_p = f(T)$
- boundary convection coefficient h = constant
- boundary radiation, emissivity $\varepsilon = f(T)$

- time steps
- node no.
- temperature

Fig. 2: Schematic diagram of the calculation

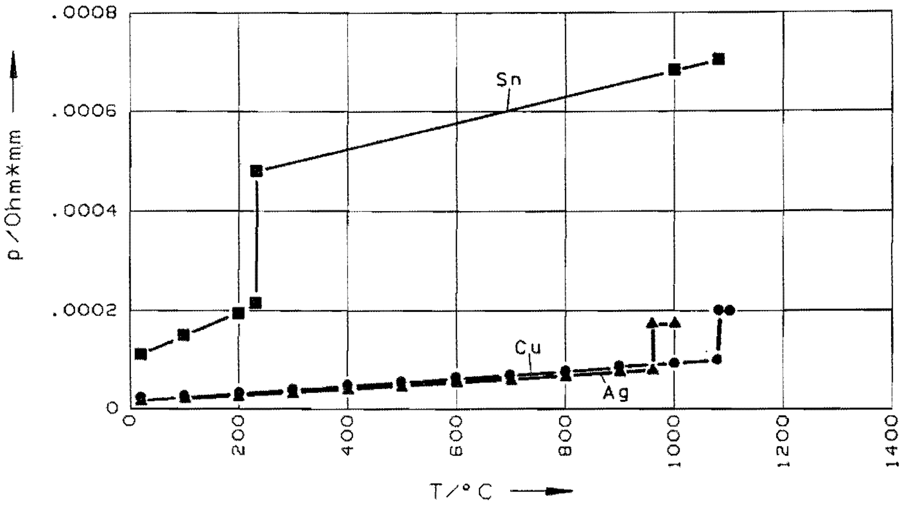

a) Specific resistance ρ as function of the temperature T

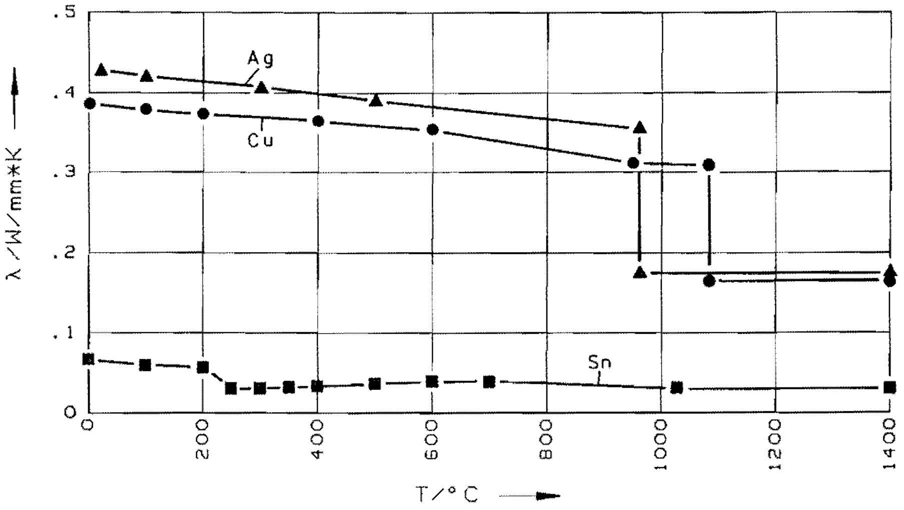

b) Heat conductivity λ as function of the temperature T

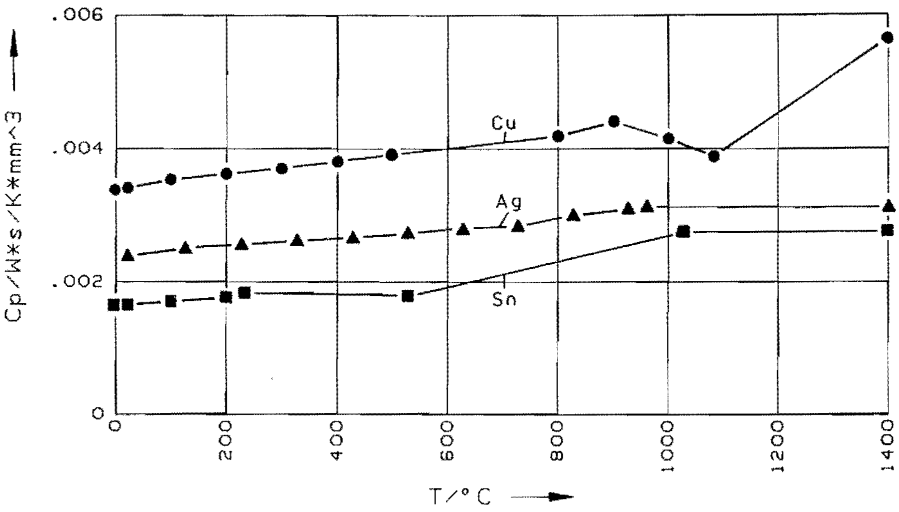

c) Heat capacity C_p as function of the temperature T

Fig. 3: Material property data of some important metals

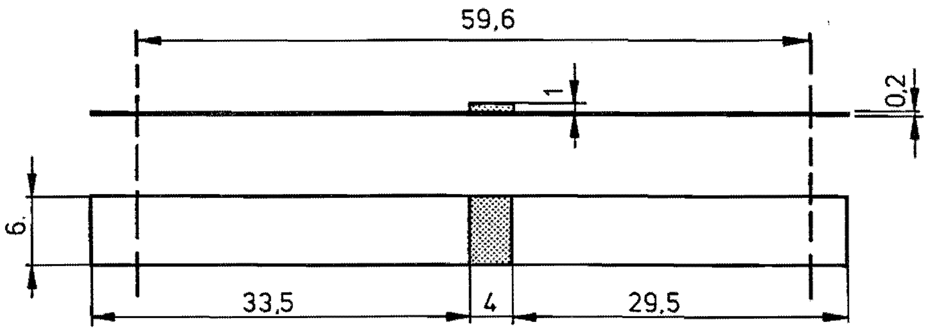

Fig. 4a: Dimensions of the straight fuse element with "M" - effect

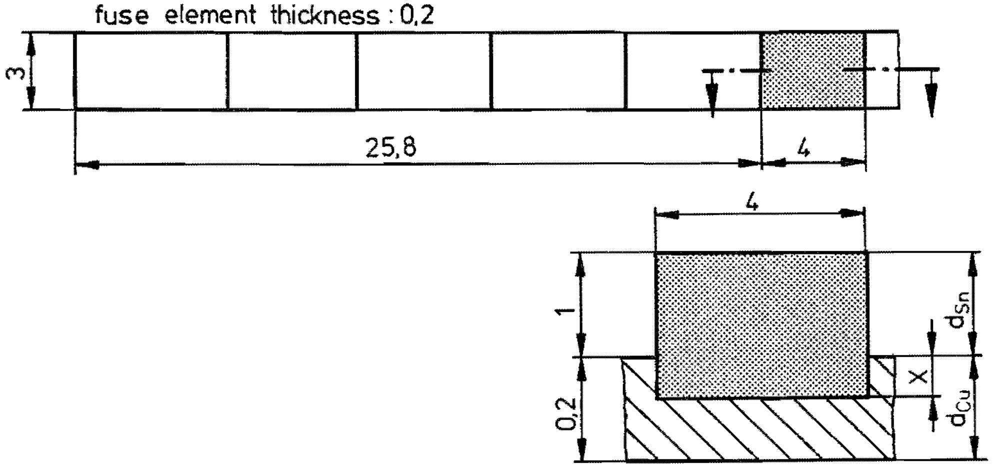

Fig. 4b: FEM - model of a straight fuse element with "M" - effect

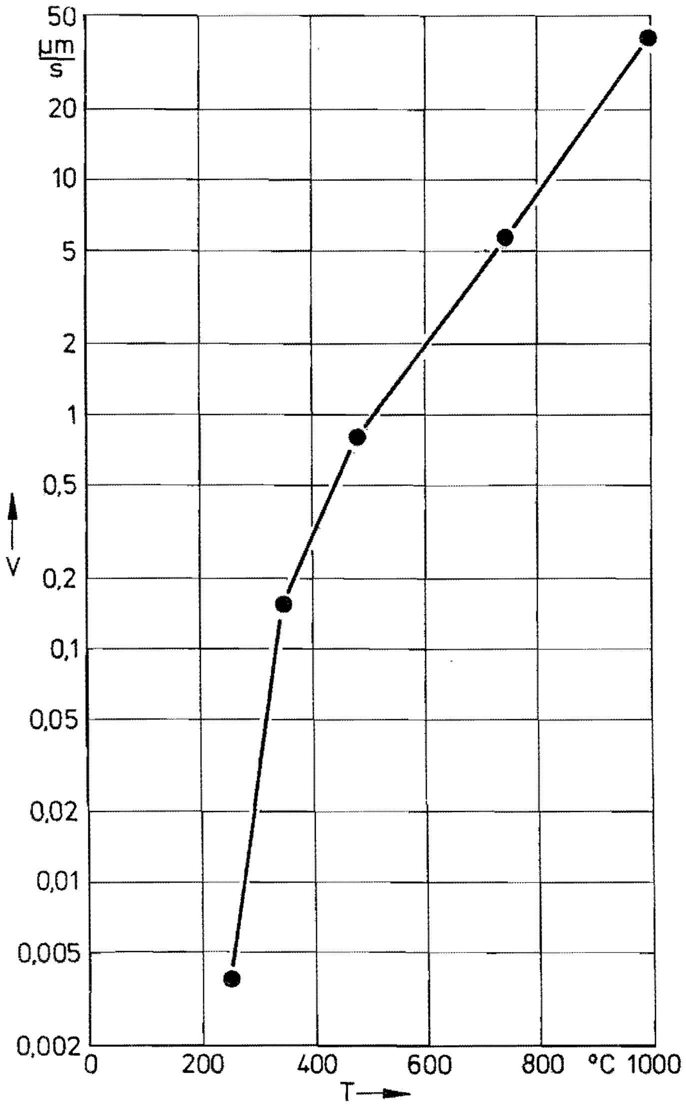

Fig. 5: Dissolution velocity v = dx/dt as function of the temperature T for Cu fuse elements with Sn solder spot

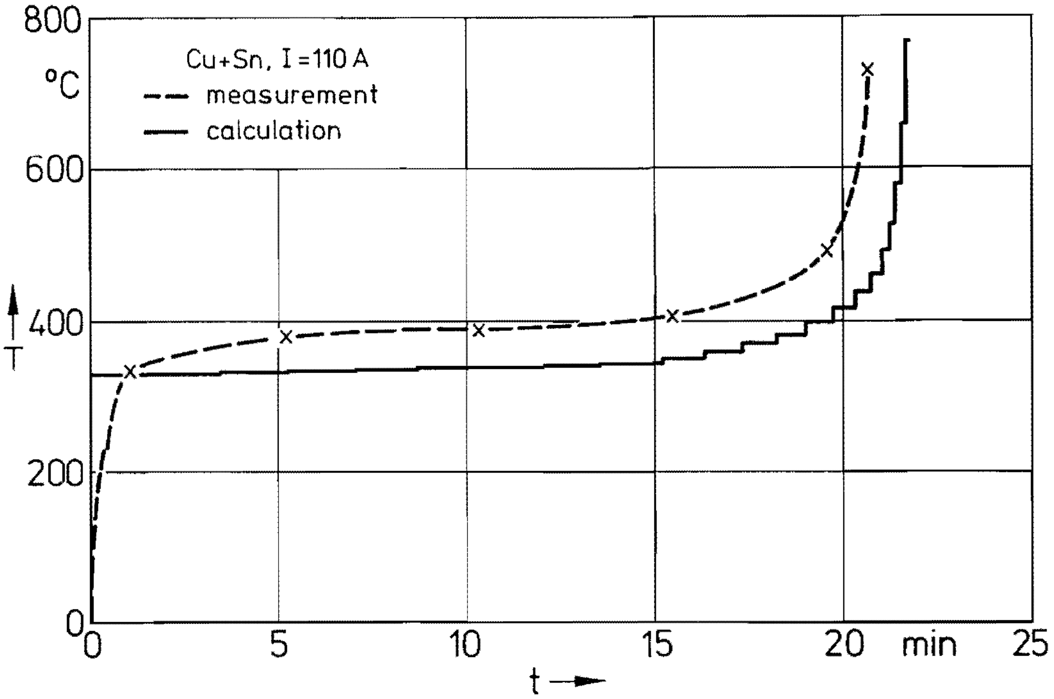

Fig. 6: Comparison of the calculated and measured temporal increase of the temperature T for Cu fuse elements with Sn solder spot at a load current I = 110 A

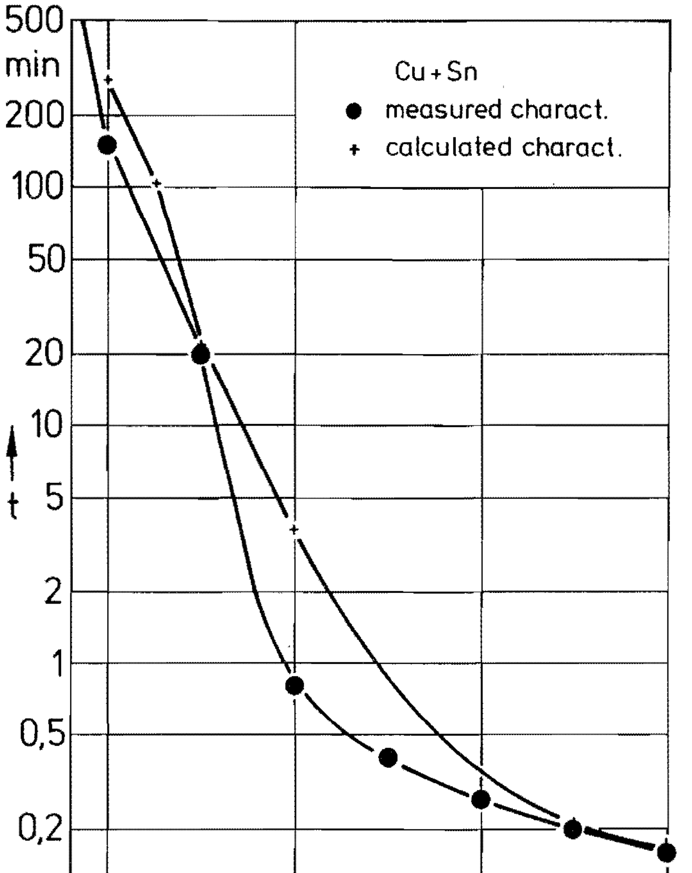

Fig. 7: Comparison of the calculated and measured time/current characteristics for the Cu fuse element with Sn solder spot